A Volcano Rekindled: The Renewed Eruption of Mount St. Helens, 2004–2006
Edited by David R. Sherrod, William E. Scott, and Peter H. Stauffer
U.S. Geological Survey Professional Paper 1750, 2008

Chapter 6

Seismicity and Infrasound Associated with Explosions at Mount St. Helens, 2004–2005

By Seth C. Moran[1], Patrick J. McChesney[2], and Andrew B. Lockhart[1]

Abstract

Six explosions occurred during 2004–5 in association with renewed eruptive activity at Mount St. Helens, Washington. Of four explosions in October 2004, none had precursory seismicity and two had explosion-related seismic tremor that marked the end of the explosion. However, seismicity levels dropped following each of the October explosions, providing the primary instrumental means for explosion detection during the initial vent-clearing phase. In contrast, explosions on January 16 and March 8, 2005, produced noticeable seismicity in the form of explosion-related tremor, infrasonic signals, and, in the case of the March 8 explosion, an increase in event size ~2 hours before the explosion. In both 2005 cases seismic tremor appeared before any infrasonic signals and was best recorded on stations located within the crater. These explosions demonstrated that reliable explosion detection at volcanoes like Mount St. Helens requires seismic stations within 1–2 km of the vent and stations with multiple acoustic sensors.

Introduction

On September 23, 2004, a swarm of volcano-tectonic earthquakes heralded the reawakening of Mount St. Helens after 18 years of quiescence (Moran and others, this volume, chap. 2). On October 1 the first small explosion occurred, with three others following over the next four days (table 1). Several of these happened during daylight hours and were broadcast on live television across the United States, perhaps creating an impression that Mount St. Helens was building towards a larger explosive eruption. Instead, these explosions were followed by the steady-state extrusion of a new dome in the southern part of the 1980 crater. The relatively steady-state extrusion was punctuated by just two explosions, one on January 16, 2005, and the other on March 8, 2005 (table 1). All six explosions were phreatic, with no evidence, such as fresh pumice, of any significant magmatic component (Scott and others, this volume, chap. 1; Rowe and others, this volume, chap. 29). Overall, the eruption in 2004–5 featured very little explosive activity, a result of the gas-poor nature of the erupted magma (Gerlach and others, this volume, chap. 26).

We use the term "explosion" in this paper to refer to an impulsive, sudden yet sustained emission of volcanic gas and pyroclasts. Rapid detection of ash-producing explosions is of paramount importance because of the demonstrated dangers posed to aircraft by airborne ash particles (for example, Neal and others, 1997). Despite the paucity of explosions, seismic and acoustic recordings of the six explosions at Mount St. Helens have yielded several important insights into the utility and placement of seismic and acoustic sensors for improved explosion-detection capabilities, as well as insights into the nature of minor explosive activity during dome-building eruptions. In this paper we present a chronology of observations and recordings of explosions from 2004–5, focusing on our ability to detect the onset and termination of each explosion and on insights gained from seismic and acoustic data into the evolution of individual explosions.

Explosions During the Vent-Clearing Phase, October 1–October 5, 2004

Explosion 1: October 1, 1202 PDT

The first explosion occurred without warning at 1202 PDT on October 1 (fig. 1*A*, table 1), 8.5 days after the start of seismic unrest (Moran and others, this volume, chap. 2). The explosion was well documented, as it took place on a clear day

[1] U.S. Geological Survey, 1300 SE Cardinal Court, Vancouver, WA 98683

[2] Pacific Northwest Seismic Network, Department of Earth and Space Sciences, University of Washington, Box 351310, Seattle, WA 98195

Table 1. Summary of eruption parameters and seismic and acoustic observations of the six explosions occurring at Mount St. Helens, Washington, during 2004–5.

[PDT, Pacific daylight (saving) time; PST, Pacific standard time.]

Explosion number, date, and time	Duration (minutes)	Seismicity before, during, and after	Infrasound detected?	Plume height (approximate, m above vent)	Eruption phase
Explosion 1: 10/01/04, 1202 PDT	19	No precursors; earthquakes stopped following onset; tremor associated with end of explosion; almost no earthquakes for several hours afterwards	N/A (no sensors)	2,400	Vent clearing
Explosion 2: 10/03/04, 2240 PDT	~25	No precursors; earthquake rates decreased after onset (drop not as pronounced as explosion 1); tremor associated with end of explosion; seismicity low following explosion	Possible, but could also be coseismic shaking	400	Vent clearing
Explosion 3: 10/04/04, 0943 PDT	~32	No precursors; earthquake rates gradually declined after onset (drop not as pronounced as explosion 2); no tremor associated with end of explosion	No	1,500	Vent clearing
Explosion 4: 10/05/04, 0905 PDT	70	No precursors; gradual but significant decline in earthquake rate and size after onset; no tremor associated with end of explosion	No	2,400	Vent clearing
Explosion 5: 01/16/05, 0312 PST	~33	No precursors; tremor occurred during entire event; no change in earthquake rate observed after explosion	Yes	Unknown	Dome building
Explosion 6: 03/08/05, 1725 PST	~20	Earthquake magnitudes increased ~2 hours before onset; tremor associated with entire event; short-lived increase in earthquake rate after explosion, rate returned to normal within 1–2 hours	Yes	9,000	Dome building

with a U.S. Geological Survey (USGS) crew flying over the crater at the start of the explosion (Schneider and others, this volume, chap. 17), and many television cameras were transmitting images live from a site near Johnston Ridge Observatory (JRO) (fig. 2) to a nationwide audience (Driedger and others, this volume, chap. 24). Infrared recordings of the base of the eruption column showed peak temperatures around 160°C, consistent with visual observations that the explosion was phreatic (Schneider and others, this volume, chap. 17). Eruption cloud tops reached ~4,500 m above sea level (asl), or 2,400 m above the vent.

As described by Moran and others (this volume, chap. 2), seismicity had intensified in a series of steps through the first several days of the crisis that began on September 23, 2004 (fig. 3). By September 29, earthquakes of magnitude 2 and greater were occurring at a rate of ~1 per minute. Although seismicity intensified gradually between 0800 and 1100 PDT on October 1, several more-rapid intensifications had occurred in the previous two days, and so this intensification was not recognized as a short-term warning sign. Because preexplosion seismicity was so intense, it was difficult to see any obvious seismicity associated with the explosion in the first several minutes after 1202 PDT (fig. 1*A*). The most obvious seismic signal was the sudden cessation of earthquakes ~1 minute after the explosion began. After the earthquakes stopped, explosion-related tremor (defined here as seismic tremor accompanying

an explosion) with frequencies of 1–3 Hz and a peak reduced displacement, or D_R (Aki and Koyanagi, 1981), of ~6 cm^2 could clearly be seen on many nearby stations (fig. 1*A*; see fig. 2 for station locations). Tremor began increasing in amplitude at 1216, then abruptly stopped at 1221, when the explosion also stopped. Weak tremor occurred again starting at 1240, but earthquakes did not occur again until ~3 hours later (Moran and others, this volume, chap. 2).

If the earthquakes had not ceased when the explosion started and the explosion had not occurred during daylight hours in clear conditions, it is possible that staff at the Cascades Volcano Observatory (CVO) and the Pacific Northwest Seismic Network (PNSN) might not have realized that an explosion had occurred. The intense earthquake activity at the time was continuously saturating nearby seismic stations, all of which had short-period vertical-component seismometers, and the explosion-related tremor would have been almost impossible to distinguish had the earthquakes not ceased. In an attempt to improve our explosion detection capability, 1-Hz infrasound-sensitive acoustic sensors (see appendix 1) were

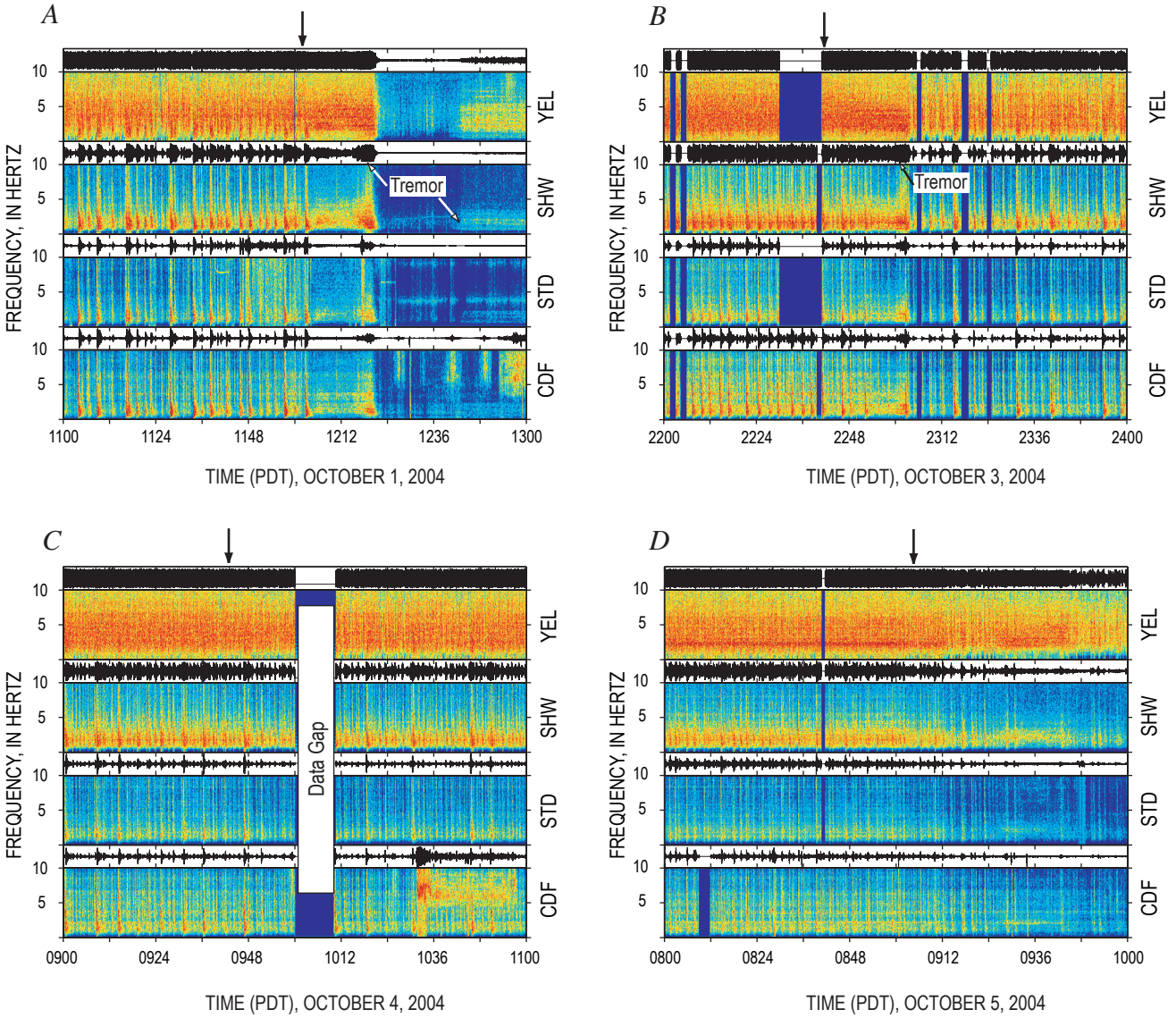

Figure 1. Multistation 2-hour-long spectrograms for explosions 1–4 at Mount St. Helens, Washington, October 2004. Time series (top) and frequency spectrogram (bottom) are shown for each of four seismic stations (see fig. 2 for station locations). Stations are shown in order of distance from vent, with closest station at top of the plot. Each time series is normalized to the maximum amplitude in each 2-hour window. Frequency spectrograms show spectral amplitudes for frequencies ranging from 0 to 10 Hz using a rainbow color palette, with dark blue corresponding to low spectral amplitudes (< 30 dB) and red to high amplitudes (>100 dB). Explosion onset time indicated by an arrow at top of each spectrogram. *A*, October 1, 2004, 1100–1300 PDT (explosion at 1202). *B*, October 3, 2004, 2200–2400 PDT (explosion at ~2240). *C*, October 4, 2004, 0900–1100 PDT (explosion at 0943). *D*, October 5, 2004, 0800–1000 PDT (explosion at 0905).

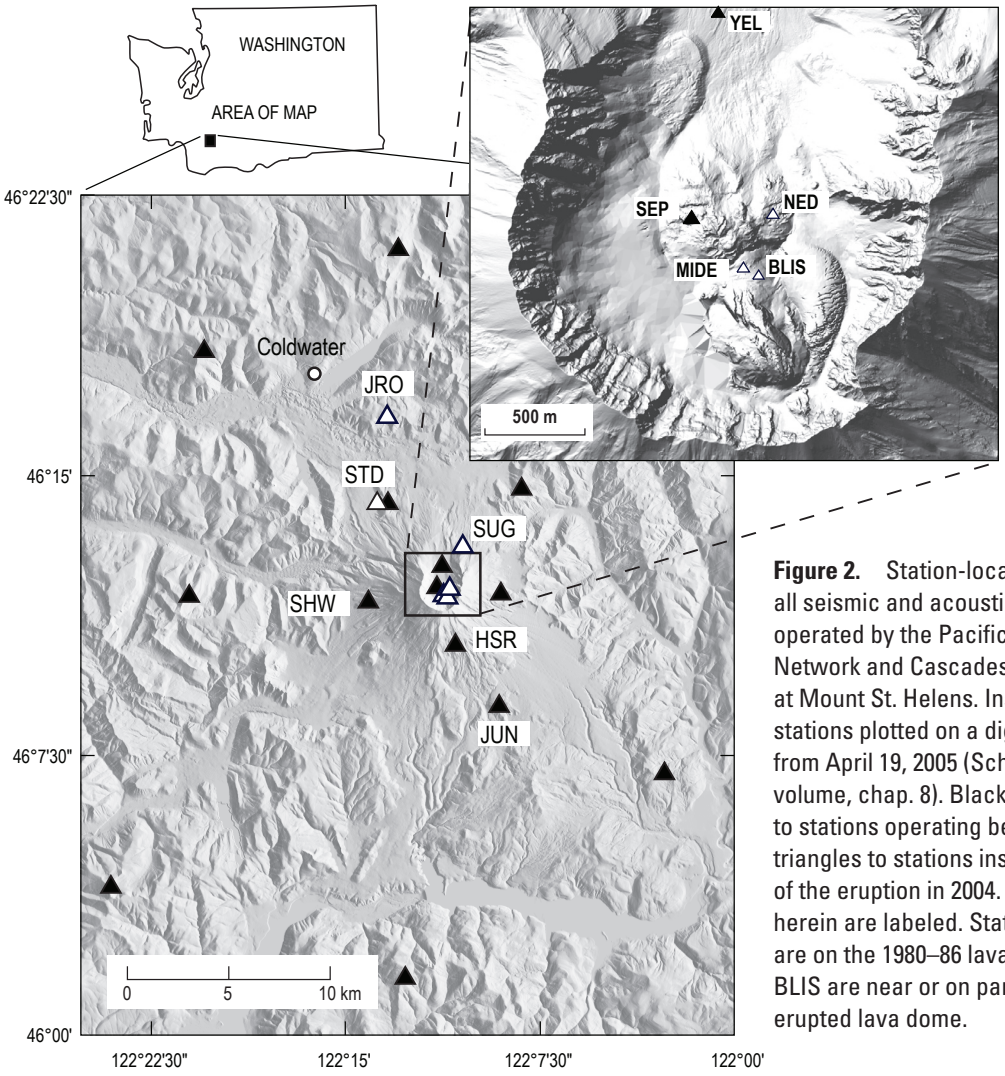

Figure 2. Station-location map showing all seismic and acoustic sensors jointly operated by the Pacific Northwest Seismic Network and Cascades Volcano Observatory at Mount St. Helens. Inset map shows stations plotted on a digital elevation model from April 19, 2005 (Schilling and others, this volume, chap. 8). Black triangles correspond to stations operating before 2004, white triangles to stations installed after the start of the eruption in 2004. All stations discussed herein are labeled. Stations SEP and NED are on the 1980–86 lava dome, MIDE and BLIS are near or on parts of the newly erupted lava dome.

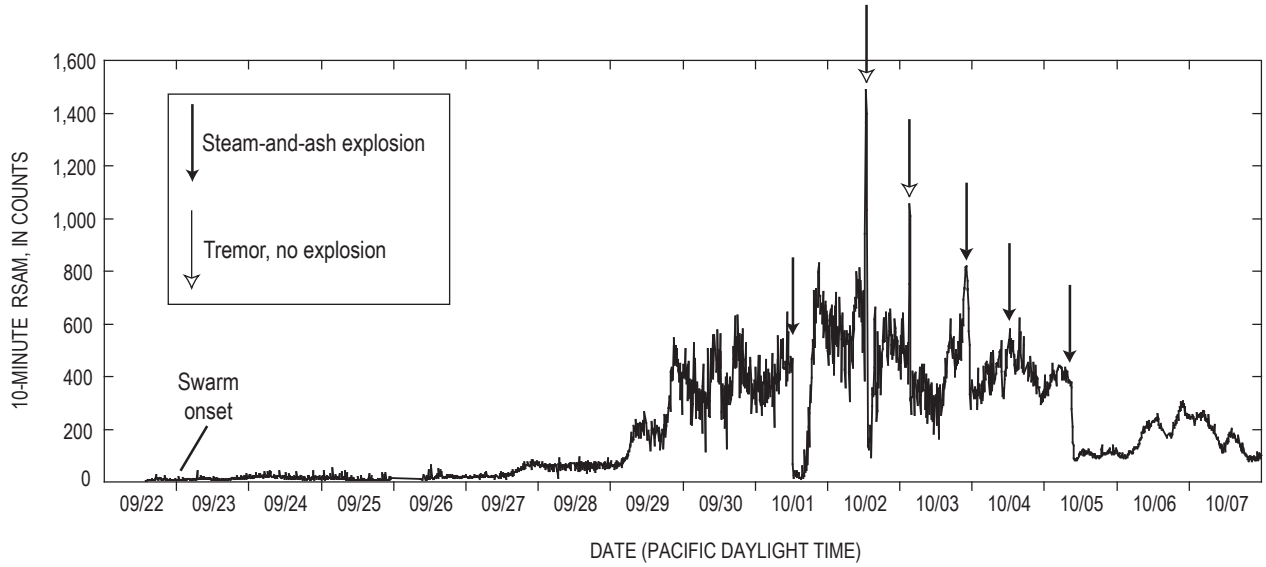

Figure 3. Plot of 10-minute RSAM values (Endo and Murray, 1991) for station SHW (see fig. 2) from September 22 to October 8, 2004. Black arrows indicate timing of individual explosions; white arrows, timing of two tremor episodes that did not correspond to any explosions (the only two such cases during entire eruption; Moran and others, this volume, chap. 2).

installed at the Studebaker Ridge station (STD) on October 2 and at Sugar Bowl (SUG) on October 3 (McChesney and others, this volume, chap. 7; see fig. 2 for station locations).

Explosion 2: October 3, ~2240 PDT

The second explosion occurred at ~2240 PDT on October 3 (fig. 1*B*). Although this explosion occurred at night, the weather was clear and U.S. Forest Service observers stationed 13 km north-northwest of the crater at the Coldwater Ridge Visitor Center reported seeing an ash cloud that barely reached the crater rim (~2,500 m asl, or 400 m above the vent) starting at ~2240 PDT (M. Guffanti, written commun., 2004). Earthquake rates and real-time seismic amplitude measurement (RSAM; Endo and Murray, 1991) levels had increased several hours before the explosion (fig. 3), and by 2100 PDT events were occurring so close together that they were difficult to distinguish, forming a spasmodic, tremorlike signal (Moran and others, this volume, chap. 2). Because there had been much more energetic tremor earlier on October 2 and October 3 with no associated explosions, the spasmodic tremor was not regarded as a short-term warning sign. As with the October 1 explosion, earthquake rates dropped significantly at ~2305 PDT following a ~3-minute-long tremor episode (peak D_R ~3 cm^2) that presumably marked the end of the explosion (fig. 1*B*). A weak, continuous acoustic signal appeared on the newly deployed microphone at STD. However, with just that single sensor, we cannot distinguish between mechanical shaking of the microphone by passing seismic waves and explosion-related infrasound. The STD microphone did record many small (~0.5 Pa) infrasonic pulses associated with M >2 earthquakes, indicating that it was sufficiently close to record weak infrasonic signals from the crater.

Explosion 3: October 4, 0943 PDT

Earthquake rates gradually increased on the morning of October 4 until the third explosion occurred at 0943 PDT (maximum plume height ~3,650 m asl, or about 1,500 m above the vent), lasting until 1015 (fig. 1*C*). The explosion was recorded by a U.S. Forest Service Web camera at the JRO and was also noted by many observers. Earthquake rates decreased following the explosion (fig. 3), although not as markedly as either of the decreases following the previous two explosions. In contrast to the October 3 explosion, no obvious signal was apparent on the acoustic sensors and no explosion-related tremor was recorded on the nearby seismic stations (fig. 1*C*). The decline in seismicity was gradual and, unlike that accompanying the October 1 explosion, did not correspond in any direct way to the onset or termination of the explosion. Given the lack of obvious associated seismic signals, it is likely that the explosion would not have been detected had it occurred during bad weather.

Dzurisin and others (2005) show in their figure 1 a second steam-and-ash explosion on October 4 at ~1400 PDT. This was based on a report of anomalous steaming in the crater at that time (M. Guffanti, written commun., 2004), a report that coincided with a small drop in RSAM values. However, subsequent review of images from the JRO Web camera (taken every five minutes; Poland and others, this volume, chap. 11) showed no obvious steam or ash plume at that time, in contrast to the 0943 explosion. Given the absence of visible ash, we consider the 1400 event, if there was an event at all, to be at most a small steam explosion that is not comparable to the confirmed explosions, and we do not consider it further in this paper.

Explosion 4: October 5, 0905 PDT

The fourth and final explosion of the vent-clearing phase occurred at 0905 PDT on October 5 and lasted until 1015 (fig. 1*D*). This was the most vigorous and long-lasting explosion of the sequence, with the ash plume reaching ~4,500 m asl (2,400 m above the vent) and depositing trace amounts of ash ~100 km from the volcano (Scott and others, this volume, chap. 1). Before the explosion, RSAM levels had increased over a 6-hour period, reaching a peak level at 0600 that was maintained until the explosion (fig. 3). Earthquake sizes and rates began declining ~15 minutes after the explosion began (fig. 1*D*), with RSAM levels falling below post-September 29 levels by the end of the explosion (fig. 3). As with the October 4 explosion, no obvious explosion-related signals were apparent either on seismic or acoustic sensors (fig. 1*D*). However, the decline in seismicity was significant enough that an explosion could have been inferred if weather conditions had prohibited observation of the explosion. A delayed indicator of the explosion was the loss of the radio signal from station YEL from 1045 to 1238 following the explosion as a result of attenuation of its radio signal by the ash cloud.

Discussion

Because there was no attempt to maintain a full-time official observer near the volcano, there is a remote possibility that other small explosions occurred between October 1 and 5 that were not detected. We feel confident that no undetected explosions occurred during daylight hours, as clear weather provided excellent viewing conditions for the mass of people and media watching the volcano from various vantage points (Driedger and others, this volume, chap. 24). During nighttime hours clear viewing conditions still existed, aided by moonlight from an almost-full moon, and, as a result, members of the public and U.S. Forest Service staff were able to see one nighttime explosion (October 3). Nevertheless, we cannot rule out the possibility that other explosions occurred at night when the volcano was not watched.

Short-term declines in seismic energy following all four explosions were perhaps the most reliable indicator that an explosion had occurred. Seismicity declines following the explosions on October 1, 3, and 5 were particularly significant (fig. 3). However, similarly significant declines followed tremor episodes on October 2 and 3, which were not associ-

ated with explosions (Moran and others, this volume, chap. 2). In addition, smaller declines similar to that following the October 4 explosion (including several on October 4) did not correspond to known explosions. Thus short-term declines in seismic energy were not, by themselves, a reliable indicator that an explosion had occurred.

Explosions During the Dome-Building Phase

Several days after the October 5, 2004, explosion, a lava spine emerged from the vent (Vallance and others, this volume, chap. 9). The rest of 2004 was dominated by lava dome construction accompanied by low gas levels (Gerlach and others, this volume, chap. 26) and regularly spaced earthquakes (Moran and others, this volume, chap. 2). During October, November, and December of 2004 we installed several seismic stations within 500 m of the vent (fig. 2) and disabled the microphone at STD, because we needed the radio telemetry channel for data from another station (McChesney and others, this volume, chap. 7). One of the new stations on the 1980–86 lava dome (SEP) had a 2-Hz three-component velocity sensor and two 1-Hz acoustic sensors spaced ~15 m apart in a north-south alignment (appendix 1), roughly radial to the vent. With two microphones we hoped to be able to use relative arrival times of signals between the two sensors to distinguish between wind gusts (which would not necessarily produce similar waveforms, but any similar waveforms would have separations of as much as several seconds between the two sensors), coseismic signals due to shaking of the microphones by passing seismic waves (which would vary depending on the coupling of each microphone to the ground), and infrasonic signals (which would produce very similar waveforms with no more than ~0.05 s difference between the two sensors).

Explosion 5: January 16, 2005, ~0312 PST

The dome-building eruption was punctuated by a relatively short-lived explosion at ~03:12:50 PST on January 16, 2005. The explosion occurred at night during poor weather and was not visually observed. It was instead signaled by the sudden onset of a continuous broadband (1–10 Hz) tremor signal (fig. 4) accompanied by several larger-than-average low-frequency (dominant frequency <5 Hz) seismic events. The explosion-related tremor was relatively small (peak D_R of ~0.5 cm^2) and did not show up well on stations outside the crater (fig. 4). As a result, preestablished amplitude-based thresholds for generating automated alarms were not exceeded (Qamar and others, this volume, chap. 3) and the explosion was not detected by CVO and PNSN staff until more than an hour later during a routine scan of seismic records.

The explosion signal initially was most obvious on station BLIS (fig. 5), located ~250 m east of the vent (fig. 2). The estimated start time for the explosion is based on the onset of tremor at BLIS. Tremor did not become obvious on other stations, including two stations located ~500 m from the vent, until it increased in amplitude starting at ~0318 (figs. 4, 5). As BLIS was close to the actively growing spine 4, the tremor signal could conceivably have been caused by rockfalls coming off the spine. Rockfalls at Mount St. Helens commonly produce spindle-shaped signals 1–2 minutes long that often only appear on nearby stations. The tremor signal on BLIS was continuous between 0312 and 0318, however, indicating that the signal was the result of a longer duration process. We speculate that this signal could have been caused by relatively weak jetting before the more significant explosion that presumably occurred in association with the increase in tremor amplitudes starting at 0318.

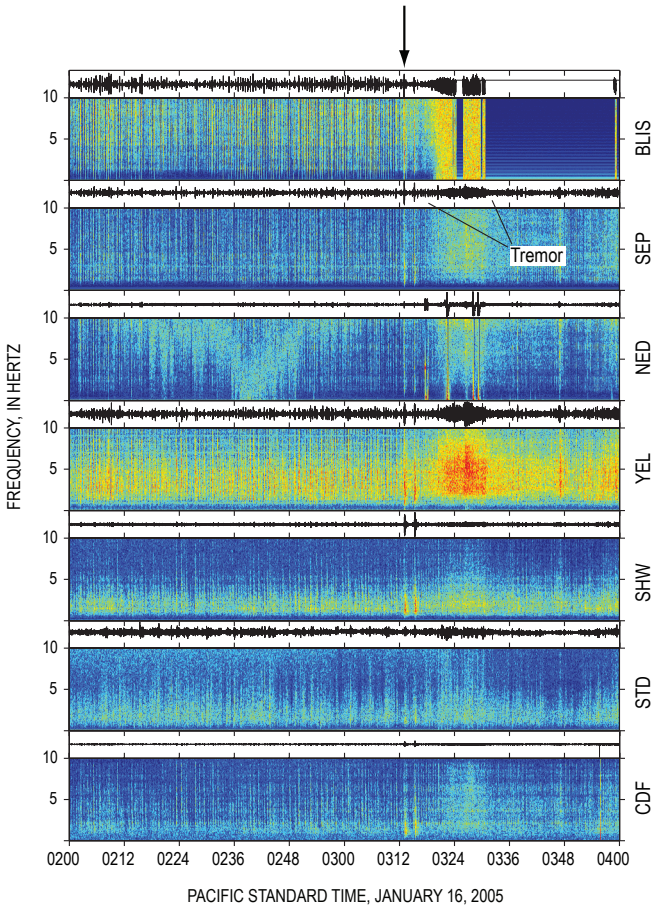

Figure 4. Multistation 2-hour-long spectrogram from 0200 to 0400 PST on January 16, 2005. See figure 2 for station locations and caption to figure 1 for description of spectrograms. Black-tipped arrow indicates estimated start time of explosion at 0312 PST; duration of tremor as seen on station SEP is indicated. Note that stations BLIS and NED had accelerometer sensors, SEP had a 2-Hz velocity sensor, and all other stations had 1-Hz velocity sensors. For more details on configuration of seismic stations, see McChesney and others (this volume, chap. 7).

Tremor rapidly intensified between 0318 and 0320. At ~0320 an emergent continuous signal became apparent on the SEP and SUG microphones (fig. 5). Given that these signals appeared in association with the seismic tremor, it is possible that some, if not most, of this signal reflects mechanical shaking of the microphones by seismic waves. We have no means of assessing this at the SUG site because it had just a single microphone and no collocated seismometer, but the near-simultaneous onset of acoustic signals at SEP and SUG suggest that at least a component of the SUG signal was due to shaking of the microphone housing. At 03:20:30, however, the two acoustic sensors at SEP began recording small-amplitude individual phases within the acoustic signals that were coherent between the two microphones and consistent with a source located at the vent. No correlative signals were apparent on the SUG acoustic sensor ~5 s later (the traveltime difference between SEP and SUG for acoustic waves traveling at 340 m/s). However, this is not surprising, given the fact that SUG is located on a ridgetop that was being buffeted by high winds from an oncoming storm system at the time. We infer that the coherent signals on the two acoustic sensors at SEP reflect the onset of explosion-related infrasound. Although the microphone recordings were still mostly incoherent at the onset of the continuous acoustic signal (fig. 5), individual phases in the signal became progressively more coherent with time. By ~0326, most of the signal was coherent and thus likely due to explosion-related infrasound (as opposed to explosion-related air currents or mechanical shaking of the sensors). The continuous acoustic signal peaked at ~0327 with maximum peak-to-peak amplitudes of 2–4 Pa (see appendix 1 for discussion of microphone calibration uncertainties) and faded to background levels by ~0331. The timing, size, duration, and character of the SEP infrasonic signals are consistent with an emergent infrasonic signal starting at 03:21:22 recorded on a microbarometer array located 13 km northwest of

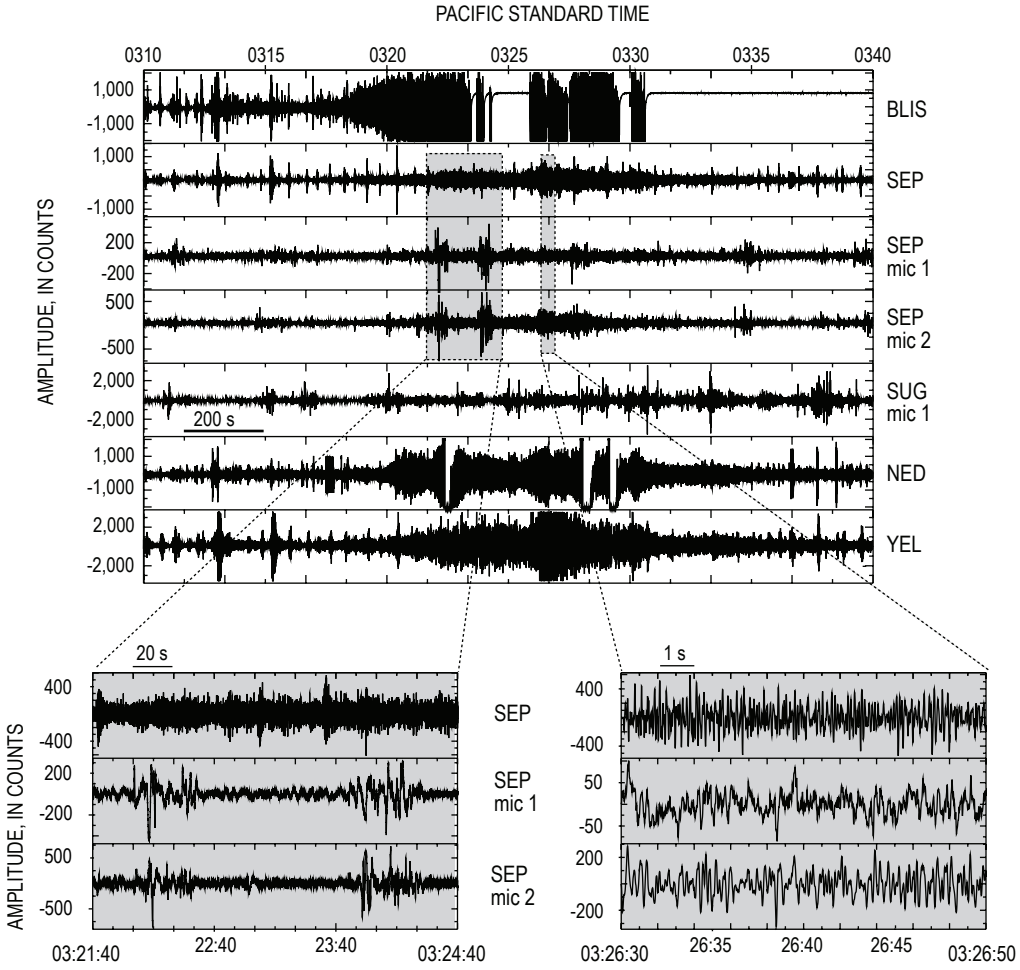

Figure 5. Multistation 30-minute plot showing unfiltered time-series data from 0310 to 0340 PST on January 16, 2005. See figure 2 for station locations. Insets at bottom of plot show 3 minutes (left) and 20 s (right) of data from vertical component of SEP seismometer (top) and two acoustic sensors (microphone 1, middle, and microphone 2, bottom), bandpass filtered with corner frequencies of 0.1 and 15 Hz. Left inset shows two events, recorded by acoustic sensors at ~03:22:00 and ~03:23:50, that we infer to be wind gusts associated with the explosion. Right inset shows mostly coherent signals between the two microphones, indicating that signals are mostly infrasonic energy produced by the explosion.

the vent near the U.S. Forest Service's Coldwater Ridge Visitor Center (Matoza and others, 2007).

Superimposed on the continuous infrasonic signal at SEP were several larger ~1 Hz pulses at 03:20:00, 03:22:05, and 03:23:50 (fig. 5). Although these pulses were broadly coherent between the two microphones, in detail the waveforms have significant variability. In addition, the time separation between relative peaks (as much as 2 s) is too large for an infrasonic signal, given the 15-m spacing of the microphones. The variability and large time differences between these pulses on the two microphones indicate that they were not traveling at sound velocities (~340 m/s) and are thus not infrasound. Other such signals were recorded in the hours before and after the explosion on both the SEP and SUG acoustic sensors, as well as at other times during stormy weather. Because a storm system was moving into the area at the time of the explosion, these pulses are likely wind gusts unrelated to the explosion. The 03:22:05 and 03:23:50 pulses, however, had larger-than-average amplitudes and broadly similar waveforms (fig. 5). On the basis of the admittedly subtle contrasts to other wind gust-related signals, we speculate that these pulses may have been caused by air flow from the explosion that swept across the SEP site at speeds of ~20 m/s.

Evidence that ash was moving across the 1980–86 lava dome shortly after the tremor-amplitude increase at 0318 comes from a several-second-long loss (or "dropout") of the radio signal from NED at 03:22:20 (fig. 5; see fig. 2 for site location). The radio signal from NED was known to be very strong. At the radio receiver for NED we measured a 30 dB fade margin—a quality determined by adding impedance at the receiver until it stops receiving the radio signal from the transmitter. The NED signal had never before been lost, even during stormy weather. The most likely explanation for the NED dropout is that the radio signal was temporarily blocked by ash. Radio telemetry was lost ~60 s later at BLIS, which had a much weaker radio signal (~10 dB fade margin at the receive site) and commonly dropped out during winter storms. Signals from both stations returned in time to record the peak of the tremor signal at 0327 (fig. 5). Shortly after this peak there were two more short-lived radio dropouts at 0328 and 0329 from station NED, followed by a dropout of several hours at station BLIS. The long duration of the BLIS dropout is consistent with a diffuse ash cloud lingering in the vent area following the explosion. Given that no dropouts occurred at SEP and that the first NED dropout occurred before the first BLIS dropout (despite BLIS being located much closer to the vent), we infer that ash was initially blown northeastwards across the dome towards NED.

Explosion-related seismic tremor gradually subsided after 0327, eventually fading to background levels at ~0345 PST on the crater stations. The tremor signal lasted for roughly 32 minutes, similar to the duration of the October 1, 2004, explosion. Subsequent geological reconnaissance on January 19 (3 days later but the first day of clear weather after the explosion) confirmed that an explosion had occurred (Scott and others, this volume, chap. 1), with the primary axis of ash deposition extending east-northeast from the vent toward both NED and BLIS (fig. 2). A field of impact craters as large as 1 m in diameter extended several hundred meters eastwards from the vent towards and beyond BLIS. Station BLIS survived in large part because it was mostly buried in snow. The distribution and thickness of deposits were similar in scope and size to those from the October 1, 2004, explosion (Scott and others, this volume, chap. 1), and it is reasonable to assume that the plume reached heights similar to the October 1 plume (~3,500–4,500 m asl).

In contrast to the October 1 explosion, nearby seismic stations were not saturated by large earthquakes before the January 16 explosion; as a result, the explosion-related tremor could clearly be seen on stations within the crater. Seismic signals from the explosion showed up poorly on stations outside the crater, however (fig. 4). If there had been no seismic stations inside the crater at the time of the explosion, it is conceivable that CVO and PNSN staff would not have known that an explosion had occurred until the next observation flight in the crater. This highlights the importance of having stations close to the vent for accurate and timely detection of explosions. In particular, the loss of telemetry on several crater stations, coupled with the tremor signal, made it clear that an ash-producing explosion had occurred.

As described above, the explosion produced infrasound that was recorded at SEP and at the Coldwater microbarometer array (Matoza and others, 2007). Had there been no crater stations, the Coldwater array might have provided the only definitive instrumental evidence that an explosion had occurred. The infrasonic signal was relatively subtle at both sites, however, and required multiple collocated acoustic sensors to distinguish between explosion-related infrasonic signals, wind noise, coseismic shaking of the acoustic sensors, and other acoustic noise sources. The subtlety of the infrasonic signals illustrates the important role that arrays of acoustic sensors can play in detecting explosions at volcanoes. Given the relatively small infrasonic signals, this explosion may represent an example of the type of ash-rich explosion that elsewhere has been found to be relatively inefficient at producing infrasound (Woulff and McGetchin, 1976; Johnson and Aster, 2005).

Explosion 6: March 8, 2005, 1725 PST

The dome-building eruption was not at all disturbed by the January 16 explosion, with earthquakes and steady-state lava-dome extrusion continuing unabated for the next seven weeks. The steady-state lava-dome extrusion was again punctuated by an explosion at ~17:25:20 PST on March 8, 2005. This was the largest of the six 2004–5 explosions; it was also the best documented and recorded of the six, as it occurred in the early evening of a cloudless day and as a result could be seen from the Portland, Oregon, metropolitan area, 85 km to the south. Tremor associated with the explosion was visible on all stations within 15 km (fig. 6), and CVO personnel who had seen the signal on seismic displays began contacting Federal, airline, and emergency officials within a minute of the start of

the explosion. Explosion-related tremor appeared simultaneously at stations inside and outside the crater and achieved maximum amplitudes (peak D_R ~1 cm^2) within the first minute, indicating that the explosion rapidly reached maximum intensity, in contrast to the January 16 explosion. Visual observations confirmed the rapid intensification, with the resultant ash plume reaching heights of about 11,000 m (9,000 m above the vent) within 5 minutes (Scott and others, this volume, chap. 1). Explosion-related tremor began declining after ~8 minutes and became indistinct from normal seismic background levels within 20 minutes. All three stations within 500 m of the vent were destroyed by the explosion (fig. 7).

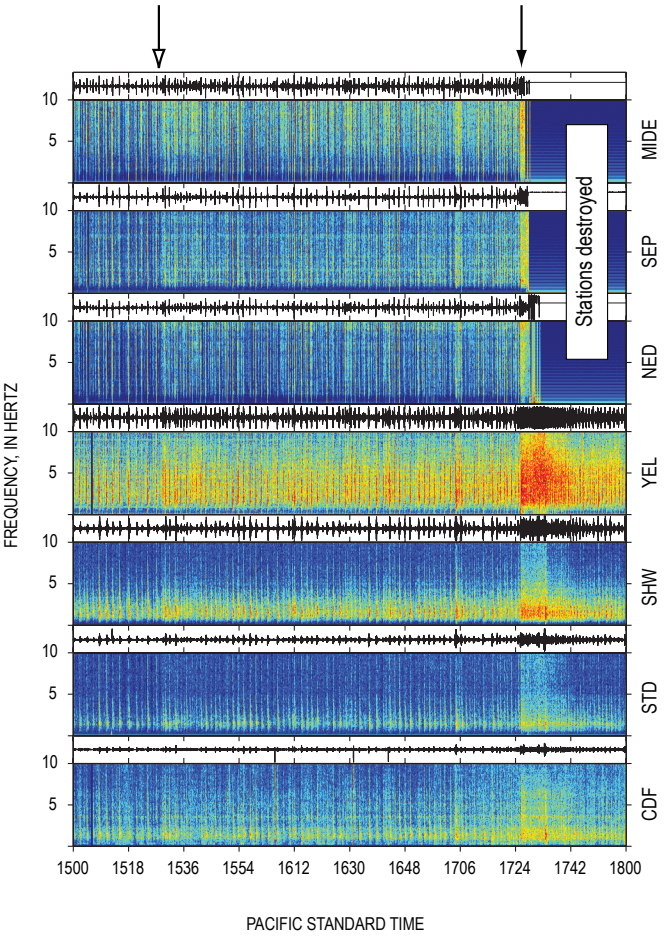

Figure 6. Multistation 3-hour-long spectrogram from March 8, 2005, between 1500 and 1800 PST. See figure 2 for station locations and caption to figure 1 for description of spectrograms. White-tipped arrow indicates start of an increase in number of larger events ~2 hour before the March 8 explosion; black-tipped arrow indicates start of explosion at 1725 PST. Note that stations MIDE and NED had accelerometer sensors, SEP had a 2-Hz velocity sensor, and all other stations had 1-Hz velocity sensors. For more details on configuration of seismic stations, see McChesney and others (this volume, chap. 7).

RSAM Increase

Roughly 2 hours before the March 8 explosion, RSAM levels began increasing at stations as far as 6 km from the vent (fig. 8). Although the increase was relatively small, particularly in comparison to increases seen in the first week of the eruption (Moran and others, this volume, chap. 2), the synchronous rise in RSAM at stations within and outside of the crater was unusual enough for CVO and PNSN staff to take notice roughly an hour before the explosion. This increase was one of the factors that contributed to the timely detection of the explosion, and it may be a relatively rare example of a short-term seismic precursor to an explosion. The RSAM increase was caused by an increase in the percentage of larger (M_d >1.5) earthquakes (fig. 9). Events in this magnitude range had been occurring at a rate of one every 3–4 minutes before the explosion. Starting at ~1529 the rate of larger events increased to one every 1–2 minutes, with the rate increasing through to the start of the explosion. No other attributes of the seismicity, including the total number of earthquakes per unit time (fig. 9), event frequency, event type, event location, and degree of similarity of waveforms between events, changed at this time.

Similar increases in event size occurred over short time intervals during the first week of seismic unrest in 2004. The fact that seismic energy levels dropped following the four explosions (particularly the October 1 and October 5, 2004, explosions) and two noneruptive tremor episodes indicates that the preexplosion elevated seismicity was a result of increased pressures in the shallow (<1 km) conduit system (Moran and others, this volume, chap. 2). We infer that the increase in seismic energy ~2 hours before the March 8 explosion similarly reflected an increase in pressure within the conduit. Given that an explosion occurred 2 hours after this increase, it is reasonable to assume that a pocket of steam and/or magmatic gas had accumulated within the conduit or along its margins at shallow depths shortly before the explosion, and that the gas pocket locally increased pressures. Given that there were no other significant changes in earthquakes before the explosion, we infer that the pressure increase merely perturbed the regular seismogenic process. Certainly, the increase in event size could reflect an increased pressurization in gas- or fluid-filled cracks (for example, Chouet, 1996). However, other factors, such as the ~1-m-thick layer of fault gouge found on most spines (Pallister and others, 2005; Cashman and others, this volume, chap. 19; Moore and others, this volume, chap. 20); the geologic evidence found for shearing within the extruded lava domes (Pallister and others, 2006); the low gas content (Gerlach and others, this volume, chap. 26); and the correlation of changes in earthquake character with changes in extrusive style at the surface (Moran and others, this volume, chap. 2), all combine to suggest that the regular earthquakes may have been a result of stick-slip motion (Iverson and others, 2006). If the earthquakes were the result of a stick-slip process, the pressure increase could have caused a seismic energy increase through (1) an increase in pressure at the base

of the plug (Iverson and others, 2006); (2) a localized increase in applied shear stress along the conduit margins; (3) a change in fault properties in the seismogenic region; or (4) some combination of these factors. Because there are no constraints on the rate of motion of the active spine or the location of the gas pocket in the hours before the explosion, there is no basis for favoring or discarding any of these explanations. Nevertheless, the increase in RSAM values shortly before the March 8 explosion represents a relatively rare instance of a seismic precursor to a volcanic explosion and provides an example of a signal that could enable future short-term forecasts of explosive events during eruptions similar to the dome-building eruption at Mount St. Helens during 2004–5.

Acoustic Recordings

In contrast to the January 16 explosion, the March 8 explosion produced significant infrasonic signals that were well recorded on the two SEP microphones (the SUG microphone had stopped working before the March 8 explosion) as well as on the Coldwater infrasound array (Matoza and others, 2007). No infrasonic signals were recorded, however, until a discrete low-frequency (1–2 Hz) pulse at 17:26:20, ~60 s after the explosion signal first appeared on seismic stations (fig. 7). We note that the delay between seismic and infrasonic signals is similar to seismicity and infrasonic observations reported by Johnson and others (2003) in association with explosions at Guagua Pichnicha volcano, Ecuador, in 1998–99. These first infrasonic pulses were low frequency (1–2 Hz) and appeared on the SEP acoustic sensors ~2 s after a seismic event was recorded on the SEP seismometer (fig. 7), consistent with the time lapse expected between seismic and acoustic waves for a source ~500 m away. Matoza and others (2007) report seeing similar infrasonic signals at their Coldwater array starting at 17:26:55, 35 s after they appeared on the SEP acoustic sensors (35 s is the expected time difference, given the 12.5-km separation between the two sites). Several similar pulses occurred over the next 20 s, followed by much larger infrasonic signals

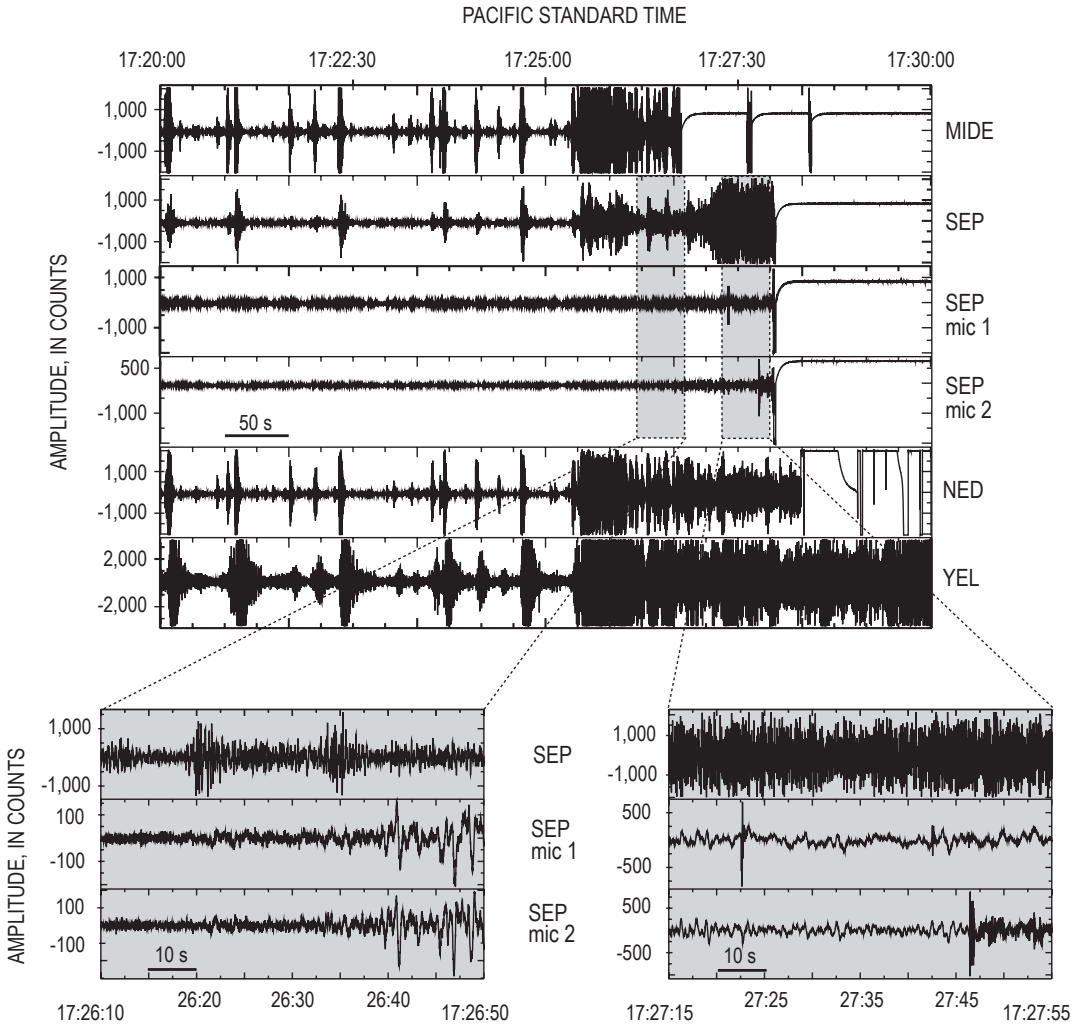

Figure 7. Multistation 10-minute plot showing time-series data from 1720 to 1730 PST on March 8, 2005. See figure 2 for station locations. Insets at bottom of plot show two 40-s windows of unfiltered data from the vertical component of the SEP seismometer (top) and two acoustic sensors (microphone 1, middle, and microphone 2, bottom). The left inset shows the onset of infrasonic signals at ~17:26:20, with amplitudes increasing significantly at ~17:26:40. Right inset shows several sharp spikes on acoustic sensors, which we infer to be caused by ballistic fragments landing close to each sensor. Conversion factor for counts to Pascals is nominally 44.5 counts/Pa for microphones at SEP (see appendix 1).

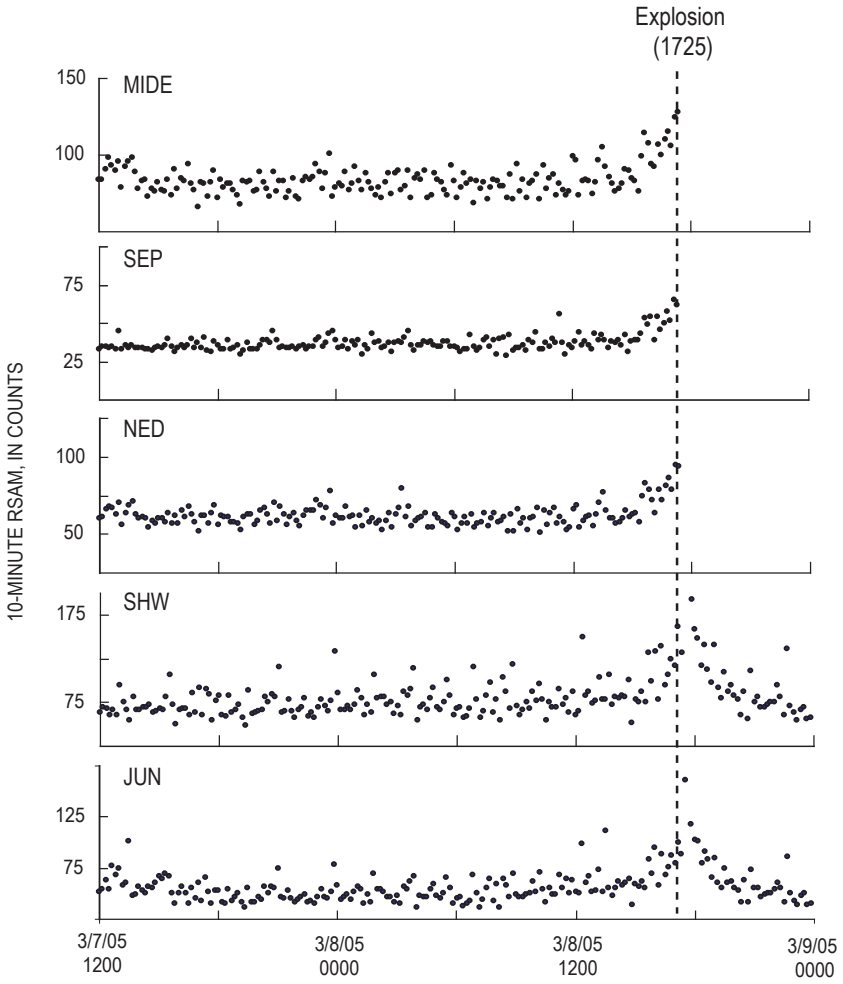

Figure 8. Plot of 10-minute RSAM values (Endo and Murray, 1991) on five stations over 36-hour time window extending from March 7 to March 9, 2005. Stations are ordered by distance from vent, nearest (MIDE, 0.25 km) to farthest (JUN, ~6.5 km). Vertical dashed line indicates start time for March 8 explosion.

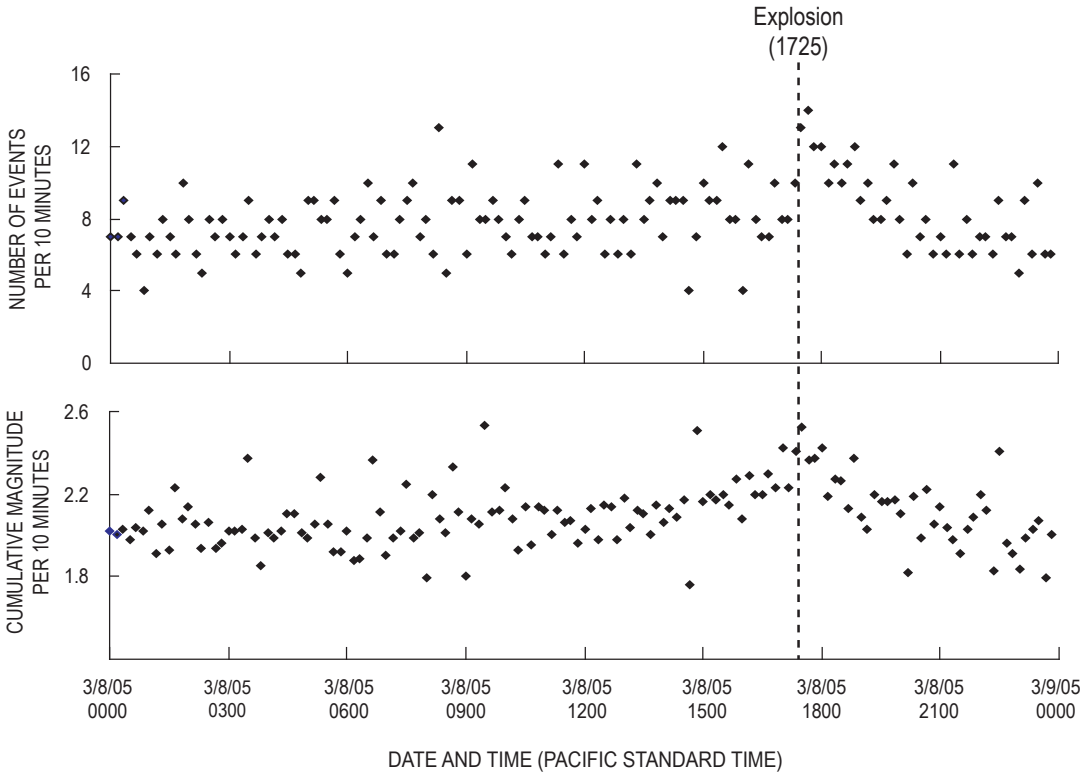

Figure 9. Plot showing number of events detected every 10 minutes at station HSR (top) and 10-minute cumulative event magnitude (bottom). Event detection is done using a standard STA/LTA trigger algorithm; for details see Moran and others (this volume, chap. 2). Event magnitudes determined using peak amplitudes at station HSR and a local magnitude relation calibrated to match the Pacific Northwest Seismic Network's coda-duration magnitude scale. Note that magnitudes began increasing slightly after 1500 PST, whereas number of events stayed constant until after explosion.

starting at 17:26:40. These larger signals were highly correlative between the two SEP acoustic sensors and did not correspond to seismic events on the SEP seismometer (fig. 7). Thus over the space of ~80 s the first phase of the explosion transitioned from producing mostly seismic signals in the first 60 s to producing both acoustic and seismic signals, and finally, 20 s later, to producing mostly acoustic signals.

Such variability in the production of acoustic and seismic energy during explosions has been documented at other volcanoes (Mori and others, 1989; Garcés and others, 1998; Johnson and others, 2003; Johnson and others, 2005; Johnson and Aster, 2005). Johnston and Aster (2005) demonstrated that this variability can be attributed to a variety of factors, including plume density, with dense plumes resulting in reduced acceleration of the atmosphere and reduced infrasonic amplitudes; magma/wall rock impedance contrast, with low impedances resulting in reduced seismic amplitudes; viscous flow in the conduit, with long and narrow conduits acting to reduce seismic and enhance infrasonic amplitudes; and source dimension, with large source regions yielding reduced infrasonic amplitudes. For the March 8 explosion, we favor an ash-rich plume as the primary reason for the apparent absence of acoustic signals in the first 60 s. Given that no open vent existed before the explosion, the initial explosion must have contained substantial amounts of ash and fractured rock mixed with steam and/or magmatic gas during the initial vent clearing. Evidence for this comes from a picture taken at 17:27:42 from a remote camera located 2.5 km northeast of the vent at SUG (fig. 10, lower photo; see fig. 2 for site location). That photograph shows a dark ash-rich cloud to the left (south) of the vent, a convecting lighter-colored plume to the right (north) that is relatively close to the SEP site, and impact craters (white patches) in snowfields on the northern side of the 1980–86 lava dome. The extent of the dark ash cloud, which enveloped most of the southern half of the crater just 140 s after the initial explosion signal (fig. 10), suggests that the initial plume contained a substantial amount of ash. The appearance of acoustic signals after 60 s could correspond to reduced ash content in the plume (and more efficient acoustic energy production) following vent clearing, with the subsequent increase in acoustic-to-seismic energy ratios over the next 20 s corresponding to progressively reduced amounts of ash entrained in the plume.

At 17:27:00 a high-frequency (>5 Hz) tremor signal that rapidly increased in amplitude appeared on the SEP seismometer (fig. 6), clipping the seismometer after 20 s. This increase was also registered at other stations within 15 km, although relative amplitude increases were much smaller, indicating that the source was close to the SEP seismometer and was likely shallow. There was no associated change in the nature or amplitude of the infrasonic signals recorded on the SEP microphones. We infer that this signal represents the generation of a second and perhaps more vigorous ash-rich plume. Although the explosion chronology is poorly detailed, photographs taken from Camas, Washington, (75 km south of Mount St. Helens), show a second plume starting to rise above the crater rim at 1727; by 1729 it had risen to the first plume's altitude at 1727 (fig. 11). The appearance of this second plume matches well with the timing of the onset of the more energetic tremor.

Further evidence for a second, more vigorous explosive phase comes from ballistic impacts. Most evidence comes from events that occurred after the tremor increase at 1727. At 17:27:22 the first of several sharp high-frequency signals appeared on the SEP microphones (fig. 7). Most of these signals appeared only on a single microphone, indicating that the source was small and very close to the sensors. We infer these to be caused by small ballistic fragments landing near individual microphones. This inference is supported by the appearance of impact craters in snow fields on the 1980–86 dome in a photo from the Sugar Bowl camera taken at 17:27:40 (fig. 10), indicating that ballistic fragments were falling at the time of the high-frequency spikes. Furthermore, the downward first-motion of the spikes (fig. 7) is inconsistent with an explosive source. We speculate that the downward first-motions might have been related to a pressure drop associated with nearby ballistic impacts. At 17:27:46, 12 s before SEP was destroyed, a low-amplitude, high-frequency signal appeared superimposed on the lower frequency infrasonic signals on both SEP microphones. On the basis of the high frequency content and small amplitude, we infer that this signal was caused by a rain of many small ballistic fragments across the SEP site. Finally, SEP and NED were both destroyed by hot ballistic fragments at 17:27:58 and 17:28:18, respectively, as indicated by multiple sharp punctures in enclosures, melted nylon ropes, and melted circuit-board solder found in equipment that was later retrieved from each site. The evidence for the bulk of ballistic impacts occurring after the tremor increase at 1727, coupled with the photographic evidence for a second plume starting at 1727, leads us to conclude that the 1727 tremor increase heralded the onset of the second and most energetic phase of the March 8 explosion.

Discussion

The explosions of 2004–5 at Mount St. Helens, although few in number and small in size, yielded a number of important insights regarding the use of acoustic and seismic instruments for reliable explosion detection, in particular for small explosions. One such insight comes from the observation that the most reliable seismic indicator for each of the four explosions occurring during the vent-clearing phase of October 1–5, 2004, was the seismicity decline following each explosion (table 1). None of the explosions had an obvious seismic precursor, and no seismic signals were recorded that heralded the start of any of the October 1–5 explosions. The lack of such obvious seismic signals may in part have been due to the intense seismicity associated with the vent-clearing phase, which would have obscured any moderate-amplitude seismic signals associated with the explosions. Despite the fact that seismicity declines followed each explosion, however,

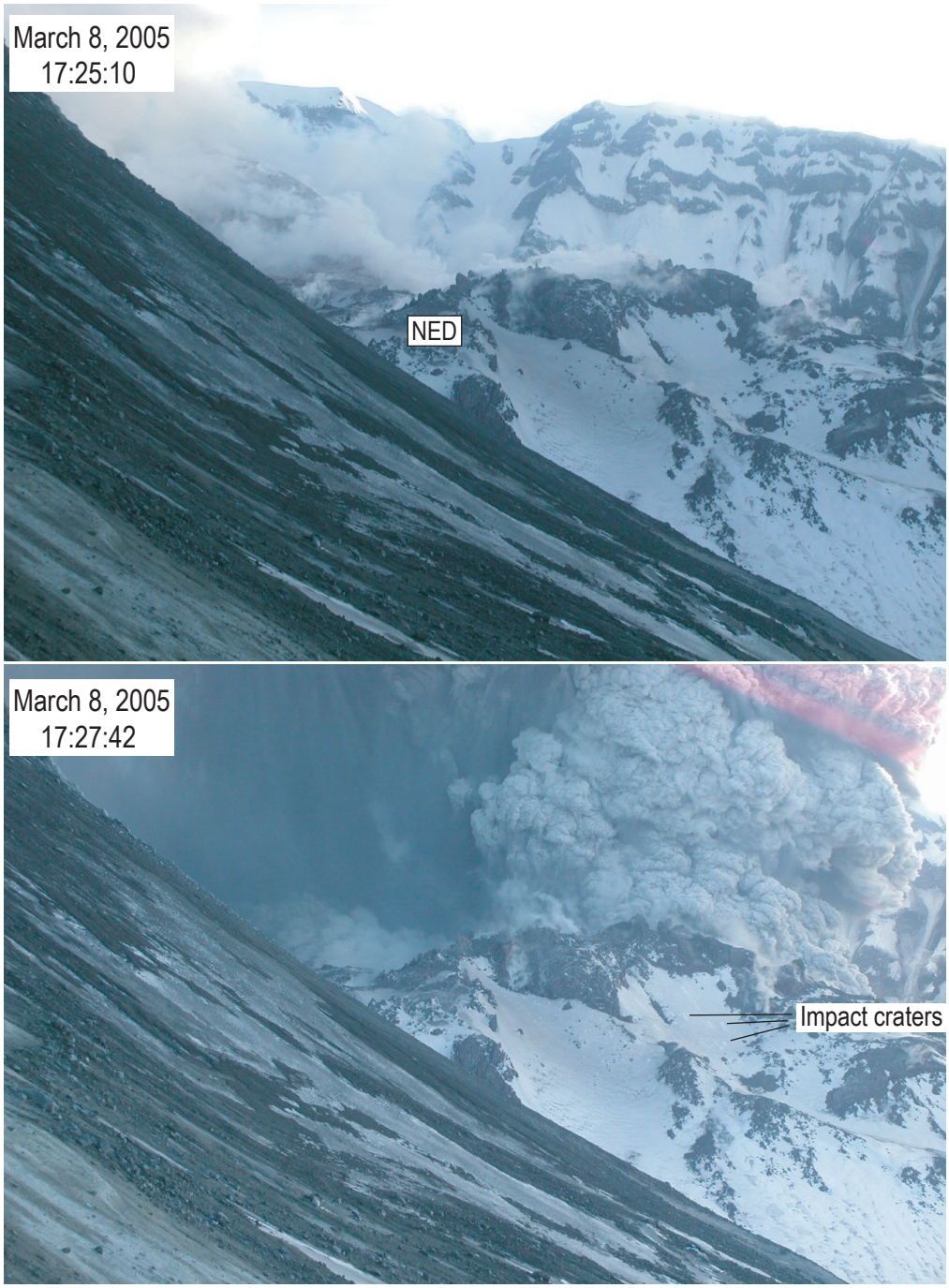

Figure 10. Photographs of the crater of Mount St. Helens taken by a remote camera installed by the Cascades Volcano Observatory at SUG (2 km northeast of vent; see fig. 2) 10 s before (top) and ~140 s after (bottom) the start of the March 8 explosion at 17:25:20 PST. Times for each photo are accurate to nearest second, because time stamps were based on a clock periodically synchronized to Internet time server. View is to south; the south crater rim is in background and the northeast crater wall in foreground. The new lava dome is mostly shrouded by steam in upper image and completely obscured by ash clouds in lower image. The 1980–86 lava dome is in the center of each image (station NED is located on northeast side of that dome). Small white circles in the snow, visible in center of lower image, formed as impact craters from ballistic fragments that fell on all sides of the 1980–86 lava dome during explosion. (Pink diagonal lines in upper right corner of lower image result from damage to the camera in previous months when sun at low zenith shone directly into lens.)

seismicity declines also occurred during this phase that did not correspond to explosions. Clearly, real-time explosion detection cannot be based on seismic instruments alone.

Another insight comes from the fact that there were no obvious acoustic signals associated with the October 3–5 explosions that occurred after two single-sensor acoustic sites were established. The lack of acoustic signals in part indicates that the explosions were not large. However, because each site had only a single acoustic sensor, it is impossible to use methods such as those employed by Matoza and others (2007) on arrays of collocated acoustic sensors to significantly reduce noise levels. As illustrated by the subsequent explosion signals recorded at SEP in 2005, multiple acoustic sensors make it much easier to distinguish between explosion-related infrasonic signals and noninfrasonic noise sources such as wind and coseismic shaking of the microphone from passing seismic waves, especially if the explosion-related signals are weak.

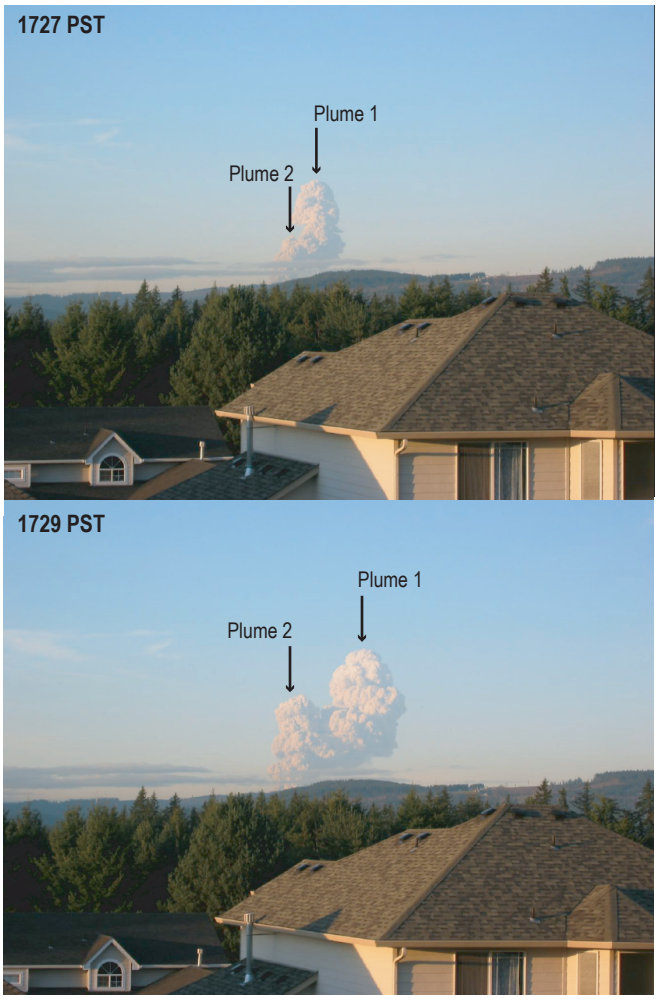

Figure 11. Views of March 8, 2005, ash cloud at 1727 and 1729 PST as seen from Camas, Washington, 75 km south of Mount St. Helens. Time for each photo is precise to nearest minute (resolution of internal clock in camera used to take these photos). Two plumes are seen clearly in lower photograph, with second plume likely corresponding to intensification in tremor seen on SEP and other seismic stations starting at 17:27:00 (see fig. 7). Given that second plume can also be seen in the 1727 photo, we estimate that the photo was taken several tens of seconds after 17:27:00. Photographs by Elisa Wells, used with permission.

The intense seismicity during the first two weeks at Mount St. Helens highlighted an additional underappreciated attribute of acoustic sensors; because they are isolated from the ground, acoustic sensors are not nearly as susceptible as seismometers to saturation by energetic seismicity and thus may record explosion-related infrasound when seismic waves from frequent large earthquakes mask any explosion-related seismicity. Although acoustic sensors deployed 3–5 km from the vent did not record obvious infrasound associated with the October 3–5 explosions, at the same time the acoustic sensors were not overwhelmed by ground waves from the continuous large earthquakes and thus were more capable of detecting explosion-related signals than the seismic network. Because vigorous precursory seismicity can happen at any volcano, acoustic sensors with real-time telemetry, in particular arrays of sensors such as those deployed at SEP and Coldwater (Matoza and others, 2007), should be installed as soon as possible after the onset of volcanic unrest to improve explosion-detection capabilities. The destruction of SEP by the March 8 explosion (and the resultant loss of acoustic information about the evolution of the explosion) also demonstrates the value in placing some acoustic arrays at safe distances, despite the greater complexity of path effects, the higher signal attenuation, and the increased time delay in explosion detection inherent in recording explosion-related signals at more distant sites.

The January 16 and March 8, 2005, explosions also demonstrated the importance of having seismic stations within 1–2 km of a vent for reliable explosion detection. Explosion-related tremor from the January 16 explosion first appeared only on a station located ~250 m from the vent and only became apparent (albeit marginally) on stations outside the crater ~8 minutes later, when infrasonic signals also became apparent on acoustic sensors. Without seismic stations operating within 1–2 km of the vent, the explosion might have gone unnoticed until later field work by CVO staff. The March 8 explosion was also recorded first by the seismic network, with infrasound signals appearing ~60 s after the start of the explosion. Given the aviation sector's stated need to be alerted within 5 minutes of the start of an eruption (Ewert and others, 2005), such delays are potentially problematic. Seismic signals were large enough to be seen on stations within 15 km of the vent, but the explosion-related tremor was most clearly recorded on crater stations. An additional benefit of having stations in the crater came from the loss of telemetry experienced at one or more crater stations during the October 1, October 5, January 16, and March 8 explosions. These dropouts provided independent confirmation that ash was in the air, and for this reason the loss of telemetry from individual sta-

tions has since become a key element in the automated alarm system employed by CVO and PNSN (Qamar and others, this volume, chap. 3). Thus, installation of real-time seismic stations within 1–2 km of a volcanic vent is vital for improving explosion-detection capabilities at erupting volcanoes.

Acknowledgments

We are indebted to Marvin Couchman for his contributions in assembling, testing, and deploying the acoustic sensors at BLIS and SEP. We also wish to acknowledge Jeff Johnson for his advice on deploying multiple acoustic sensors at SEP; Robin Matoza and Michael Hedlin for generously sharing data and interpretations of acoustic signals recorded at their Coldwater infrasonic site; Mike Poland for having the foresight to install the Sugar Bowl camera in October 2004; Rick LaHusen, for maintaining the camera and associated telemetry system in the months after Mike's move to the Hawaiian Volcano Observatory; and Elisa Wells (wife of S. Moran) for having the presence of mind to start taking photos of the March 8, 2005, explosion cloud and for allowing us to publish them. Finally, we gratefully acknowledge Jackie Caplan-Auerbach and Jeff Johnson for their thoughtful and helpful reviews of this paper.

References Cited

Aki, K., and Koyanagi, R.Y., 1981, Deep volcanic tremor and magma ascent mechanism under Kilauea, Hawaii: Journal of Geophysical Research, v. 86, p. 7095–7110.

Cashman, K.V., Thornber, C.R., and Pallister, J.S., 2008, From dome to dust; shallow crystallization and fragmentation of conduit magma during the 2004–2006 dome extrusion of Mount St. Helens, Washington, chap. 19 *of* Sherrod, D.R., Scott, W.E., and Stauffer, P.H., eds., A volcano rekindled; the renewed eruption of Mount St. Helens, 2004–2006: U.S. Geological Survey Professional Paper 1750 (this volume).

Chouet, B.A., 1996, Long-period volcano seismicity; its source and use in eruption forecasting: Nature, v. 380, p. 309–316.

Driedger, C.L., Neal, C.A., Knappenberger, T.H., Needham, D.H., Harper, R.B., and Steele, W.P., 2008, Hazard information management during the autumn 2004 reawakening of Mount St. Helens volcano, Washington, chap. 24 *of* Sherrod, D.R., Scott, W.E., and Stauffer, P.H., eds., A volcano rekindled; the renewed eruption of Mount St. Helens, 2004–2006: U.S. Geological Survey Professional Paper 1750 (this volume).

Dzurisin, D., Vallance, J.W., Gerlach, T.M., Moran, S.C., and Malone, S.D., 2005, Mount St. Helens reawakens: Eos (American Geophysical Union Transactions), v. 86, no. 3, p. 25, 29.

Endo, E.T., and Murray, T., 1991, Real-time seismic amplitude measurement (RSAM); a volcano monitoring and prediction tool: Bulletin of Volcanology, v. 53, no. 7, p. 533–545.

Ewert, J.W., Guffanti, M., and Murray, T.L., 2005, An assessment of volcanic threat and monitoring capabilities in the United States; framework for a National Volcano Early Warning System: U.S. Geological Survey Open-File Report 2005–1164, 62 p.

Garcés, M.A., Hagerty, M.T., and Schwartz, S.Y., 1998, Magma acoustics and time-varying melt properties at Arenal Volcano, Costa Rica: Geophysical Research Letters, v. 25, p. 2293–2296.

Gerlach, T.M., McGee, K.A., and Doukas, M.P., 2008, Emission rates of CO_2, SO_2, and H_2S, scrubbing, and preeruption excess volatiles at Mount St. Helens, 2004–2005, chap. 26 *of* Sherrod, D.R., Scott, W.E., and Stauffer, P.H., eds., A volcano rekindled; the renewed eruption of Mount St. Helens, 2004–2006: U.S. Geological Survey Professional Paper 1750 (this volume).

Iverson, R.M., Dzurisin, D., Gardner, C.A., Gerlach, T.M., LaHusen, R.G., Lisowski, M., Major, J.J., Malone, S.D., Messerich, J.A., Moran, S.C., Pallister, J.S., Qamar, A.I., Schilling, S.P., and Vallance, J.W., 2006, Dynamics of seismogenic volcanic extrusion at Mount St. Helens in 2004–05: Nature, v. 444, no. 7118, p. 439–443, doi:10.1038/nature05322.

Johnson, J.B., and Aster, R.C., 2005, Relative partitioning of acoustic and seismic energy during Strombolian eruptions: Journal of Volcanology and Geothermal Research, v. 148, p. 334–354.

Johnson, J.B., Aster, R.C., Ruiz, M.C., Malone, S.D., McChesney, P.J., Lees, J.M., and Kyle, P.R., 2003, Interpretation and utility of infrasonic records from erupting volcanoes: Journal of Volcanology and Geothermal Research, v. 121, p. 15–63.

Johnson, J.B., Ruiz, M.C., Lees, J.M., and Ramon, P., 2005, Poor scaling between elastic energy release and eruption intensity at Tungurahua Volcano, Ecuador: Geophysical Research Letters, v. 32, L15304, 5 p., doi:10.1029/2005GL022847.

Matoza, R.S., Hedlin, M.A.H., and Garcés, M.A., 2007, An infrasound array study of Mount St. Helens: Journal of Volcanology and Geothermal Research, v. 160, p. 249–262, doi:10.1016/j.jvolgeores.2006.10.006.

McChesney, P.J., 1999, McVCO handbook 1999: U.S. Geological Survey Open-File Report 99–361, 48 p. [http://wrgis.wr.usgs.gov/open-file/of99-361.]

McChesney, P.J., Couchman, M.R., Moran, S.C., Lockhart, A.B., Swinford, K.J., and LaHusen, R.G., 2008, Seismic-monitoring changes and the remote deployment of seismic stations (seismic spider) at Mount St. Helens, 2004–2005, chap. 7 *of* Sherrod, D.R., Scott, W.E., and Stauffer, P.H., eds., A volcano rekindled; the renewed eruption of Mount St. Helens, 2004–2006: U.S. Geological Survey Professional Paper 1750 (this volume).

Moore, P.L., Iverson, N.R., and Iverson, R.M., 2008, Frictional properties of the Mount St. Helens gouge, chap. 20 *of* Sherrod, D.R., Scott, W.E., and Stauffer, P.H., eds., A volcano rekindled; the renewed eruption of Mount St. Helens, 2004–2006: U.S. Geological Survey Professional Paper 1750 (this volume).

Mori, J., Patia, H., McKee, C., Itikarai, I., Lowenstein, P., De Saint Ours, P., and Talai, B., 1989, Seismicity associated with eruptive activity at Langila Volcano, Papua New Guinea: Journal of Volcanology and Geothermal Research, v. 38, p. 243–255.

Moran, S.C., Malone, S.D., Qamar, A.I., Thelen, W.A., Wright, A.K., and Caplan-Auerbach, J., 2008, Seismicity associated with renewed dome building at Mount St. Helens, 2004–2005, chap. 2 *of* Sherrod, D.R., Scott, W.E., and Stauffer, P.H., eds., A volcano rekindled; the renewed eruption of Mount St. Helens, 2004–2006: U.S. Geological Survey Professional Paper 1750 (this volume).

Neal, C.A., Casadevall, T.J., Miller, T.P., Hendley, J.W., II, and Stauffer, P.H., 1997, Volcanic ash—danger to aircraft in the North Pacific: U.S. Geological Survey Fact Sheet 030–97, 2 p.

Pallister, J.S., Reagan, M., and Cashman, K., 2005, A new eruptive cycle at Mount St. Helens?: Eos (American Geophysical Union Transactions), v. 87, no. 48, p. 499–500, doi:10.1029/2005EO480006.

Pallister, J.S., Hoblitt, R., Denlinger, R., Sherrod, D., Cashman, K., Thornber, C., and Moran, S., 2006, Structural geology of the Mount St. Helens fault-gouge-zone field relations along the volcanic conduit-wallrock interface [abs.]: Eos (American Geophysical Union Transactions), v. 87, no. 52, Fall Meeting supplement, Abstract V41A-1703.

Poland, M.P., Dzurisin, D., LaHusen, R.G., Major, J.J., Lapcewich, D., Endo, E.T., Gooding, D.J., Schilling, S.P., and Janda, C.G., 2008, Remote camera observations of lava dome growth at Mount St. Helens, Washington, October 2004 to February 2006, chap. 11 *of* Sherrod, D.R., Scott, W.E., and Stauffer, P.H., eds., A volcano rekindled; the renewed eruption of Mount St. Helens, 2004–2006: U.S. Geological Survey Professional Paper 1750 (this volume).

Qamar, A.I., Malone, S.D., Moran, S.C., Steele, W.P., and Thelen, W.A., 2008, Near-real-time information products for Mount St. Helens—tracking the ongoing eruption, chap. 3 *of* Sherrod, D.R., Scott, W.E., and Stauffer, P.H., eds., A volcano rekindled; the renewed eruption of Mount St. Helens, 2004–2006: U.S. Geological Survey Professional Paper 1750 (this volume).

Rowe, M.C., Thornber, C.R., and Kent, A.J.R., 2008, Identification and evolution of the juvenile component in 2004–2005 Mount St. Helens ash, chap. 29 *of* Sherrod, D.R., Scott, W.E., and Stauffer, P.H., eds., A volcano rekindled; the renewed eruption of Mount St. Helens, 2004–2006: U.S. Geological Survey Professional Paper 1750 (this volume).

Schilling, S.P., Thompson, R.A., Messerich, J.A., and Iwatsubo, E.Y., 2008, Use of digital aerophotogrammetry to determine rates of lava dome growth, Mount St. Helens, Washington, 2004–2005, chap. 8 *of* Sherrod, D.R., Scott, W.E., and Stauffer, P.H., eds., A volcano rekindled; the renewed eruption of Mount St. Helens, 2004–2006: U.S. Geological Survey Professional Paper 1750 (this volume).

Schneider, D.J., Vallance, J.W., Wessels, R.L., Logan, M., and Ramsey, M.S., 2008, Use of thermal infrared imaging for monitoring renewed dome growth at Mount St. Helens, 2004, chap. 17 *of* Sherrod, D.R., Scott, W.E., and Stauffer, P.H., eds., A volcano rekindled; the renewed eruption of Mount St. Helens, 2004–2006: U.S. Geological Survey Professional Paper 1750 (this volume).

Scott, W.E., Sherrod, D.R., and Gardner, C.A., 2008, Overview of the 2004 to 2006, and continuing, eruption of Mount St. Helens, Washington, chap. 1 *of* Sherrod, D.R., Scott, W.E., and Stauffer, P.H., eds., A volcano rekindled; the renewed eruption of Mount St. Helens, 2004–2006: U.S. Geological Survey Professional Paper 1750 (this volume).

Vallance, J.W., Schneider, D.J., and Schilling, S.P., 2008, Growth of the 2004–2006 lava-dome complex at Mount St. Helens, Washington, chap. 9 *of* Sherrod, D.R., Scott, W.E., and Stauffer, P.H., eds., A volcano rekindled; the renewed eruption of Mount St. Helens, 2004–2006: U.S. Geological Survey Professional Paper 1750 (this volume).

Woulff, G., and McGetchin, T.R., 1976, Acoustic noise from volcanoes; theory and experiment: Geophysical Journal of the Royal Astronomic Society, v. 45, p. 601–616.

Appendix 1. Acoustic Sensors Used at Mount St. Helens

The acoustic sensors installed by CVO and PNSN at Mount St. Helens were previously designed as additions to the McVCO voltage-controlled oscillator (McChesney, 1999) that is in wide use by the PNSN and the USGS in the Cascades and elsewhere. The sensor consists of either 9 or 18 electret microphones with a 1-Hz frequency response, the signals from all microphones being summed to reduce electronic noise. Including the responses of other components in the recording system (for example, radio, digitizers, system gain), each 9-element microphone has a nominal response of 22.7 counts/Pascal (44.5 counts/Pascal for an 18-element microphone). The acoustic sensors installed at stations SEP and SUG had 18-element microphones, and the STD sensor had a 9-element microphone. An important caveat to the acoustic response of these sensors is that individual sensors were not calibrated before installation. Given that the sensitivity of individual electret sensors varies by ±3 dB and that their sensitivity is known to decline with time after installation (depending on environmental conditions), we estimate that the true response could vary by 30 percent or more for each nine-element microphone. For this reason we only give a range of possible pressure values in this paper.

The circuit board with electret sensors is typically placed in a PVC plastic tube with end caps and a hose connection on one end. The PVC tubing reduces bellows-type motion caused by wind or ground shaking. A soaker hose of variable length is attached to the hose connection to further reduce wind noise. At SUG and STD the sensors were placed inside an enclosure with the soaker hose strung in a line away from the enclosure. At SEP the two sensors were placed on the ground ~15 m apart, with rocks piled around the PVC tube to prevent movement and the soaker hose coiled next to each sensor.